Uranyl Ion Complexes of Polycarboxylates: Steps towards Isolated Photoactive Cavities

Jack Harrowfield, Pierre Thuéry

chemistry

MDPI

Review

Uranyl Ion Complexes of Polycarboxylates: Steps towards Isolated Photoactive Cavities

Jack Harrowfield [1,*] and Pierre Thuéry [2,*]

[1] Institut de Science et d'Ingénierie Supramoléculaires, Université de Strasbourg, 8 allée Gaspard Monge, 67083 Strasbourg, France

[2] Université Paris-Saclay, CEA, CNRS, NIMBE, 91191 Gif-sur-Yvette, France

* Correspondence: harrowfield@unistra.fr (J.H.); pierre.thuery@cea.fr (P.T.)

Received: 29 January 2020; Accepted: 18 February 2020; Published: 20 February 2020

Abstract: Consideration of the extensive family of known uranyl ion complexes of polycarboxylate ligands shows that there are quite numerous examples of crystalline solids containing capsular, closed oligomeric species with the potential for use as selective heterogeneous photo-oxidation catalysts. None of them have yet been assessed for this purpose, and some have obvious deficiencies, although related framework species have been shown to have the necessary luminescence, porosity and, to some degree, selectivity. Aspects of ligand design and complex composition necessary for the synthesis of uranyl ion cages with appropriate luminescence and chemical properties for use in selective photo-oxidation catalysis have been analysed in relation to the characteristics of known capsules.

Keywords: uranium(VI); carboxylates; capsules; structure; luminescence

1. Introduction

Intensive research over the past few decades has been devoted to the synthesis of crystalline cavity-containing, framework, and coordination polymer species of a porous nature suited to the storage, immobilisation, sensing, or reaction of a wide variety of substrates of environmental and economic importance [1–15]. (The references cited here are a somewhat eclectic selection intended to illustrate the range of chemistry involved, rather than to be comprehensive, which is far from the case.) This has resulted not only in real advances towards practical objectives in gas storage [1,5,16,17] but also in unanticipated developments such as that of the "crystalline sponge" method [18,19] of determining the molecular structures of molecules otherwise difficult to crystallise. While metal ions clearly have a fundamental role in determining the structure of these materials, of equal importance is that they endow the solids with functionality specific to the given metal ion. One such function is that of photoactivity, a property which may have various manifestations [2,8], but which in the case of uranium(VI) as uranyl ion, UO_2^{2+}, derivatives, is anticipated to be that of photo-oxidation catalysis, long known in their solution chemistry [20–22].

Although photocatalysis by metal-organic framework (MOF) systems in particular could be described in 2017 as a "largely unexplored field" [23], it has rapidly become a popular area of study [24]. Investigations of hetereogeneous photocatalysis by uranyl-containing solids [25–35], however, have remained largely limited to those of oxidative destruction of environmental pollutants or to basic mechanistic work, although water splitting has been frequently cited as a possible application. Selectivity of these reactions has not been a major focus and in some early instances [34] would be expected to have been determined by the nature of the preformed support upon which uranyl centres were immobilised. Given that the use of a radioactive material would pose problems in any large-scale application for environmental remediation or water splitting, an alternative, more appealing prospect is that of selective photochemical synthesis within cavities of a porous uranyl

complex crystal, a prospect which parallels what has already been realised for synthesis in general with other metal ion derivatives [2,36–38] and which is rendered worthy of wider investigation by the observation of selective incorporation of various materials into the cavities of some known uranyl ion coordination polymers [39–45].

In general, polycarboxylates, often in the company of aza-aromatic species, are the most important class of ligands giving rise to coordination polymers, metal-organic frameworks, and closed metallo-clusters [1–14,46]. This is particularly true of uranyl ion containing systems [30,47–51], and it is for this reason that the present report is focussed upon uranyl polycarboxylates, though this is not to say that less-investigated species such as, for example, those based on polyphosphonates [52–55] are not of equal potential interest. We do note, however, that while uranyl ion photocatalysed oxidation of carboxylic acids is a long known reaction [20,21], it is slow and there is little evidence that the synthesis of uranyl carboxylates [49] is significantly influenced by it, so that the extraordinary variety of known carboxylate systems is open to exploration. With the particular objective of defining possibly more efficient pathways to photoactive closed uranyl-polycarboxylate oligomers, expected to be the most stringent form of receptor, we present an analysis of both positive and negative aspects of the crystal structures and composition of currently known system.

2. Discussion

The first closed uranyl polycarboxylate oligomer to be structurally characterised [56] was that formed by a monoester derivative of the *cis*,*trans* stereoisomer of 1,3,5-trimethylcyclohexane-1,3,5-tricarboxylic acid in its dianionic form (L^{2-}) and with the composition $(HNEt_3)_8[(UO_2)_8(L)_8(O_2)_4]\cdot 5CHCl_3\cdot 16H_2O\cdot 6CH_3OH$ (**A**, CSD refcode GOPVUC). The box-like, octa-anionic oligomer found in this structure (Figure 1) defines a cavity large enough to accommodate two triethylammonium cations and (partly) two chloroform molecules, indicating that small molecule reactions within the cavity could be possible provided the cations could be replaced by reactive species. It also has features found in many other uranyl complexes in that the carboxylate groups are bound as κ^2O,O' chelates and the peroxide ligands act as bridges to produce convergent $U(O_2)U$ units. The adventitious presence of peroxide in the complex is not an unusual observation in uranyl ion coordination chemistry and detailed studies [57,58] have led to its rationalisation as a result of photochemical reduction of uranyl ion by water or organic substrates (such as methanol) to give U(V), which subsequently reacts with atmospheric oxygen to give peroxide. The bent form of the $U(O_2)U$ unit is favourable for the formation of a closed species and this effect is spectacularly exemplified in the extraordinary family of cages formed by uranyl ion in the presence of peroxide ion and various co-ligands such as oxide, hydroxide, nitrate, phosphate and other simple oxyanions, a family known to extend up to a multi-compartmental cage built from 124 uranyl units [59,60]. The presence of bound peroxide on uranyl ion, however, has the unfortunate consequence that uranyl ion emission, with its characteristic multiple vibronic components [21,61], is quenched, though ligand-centred emission is observed in some cases [58,62].

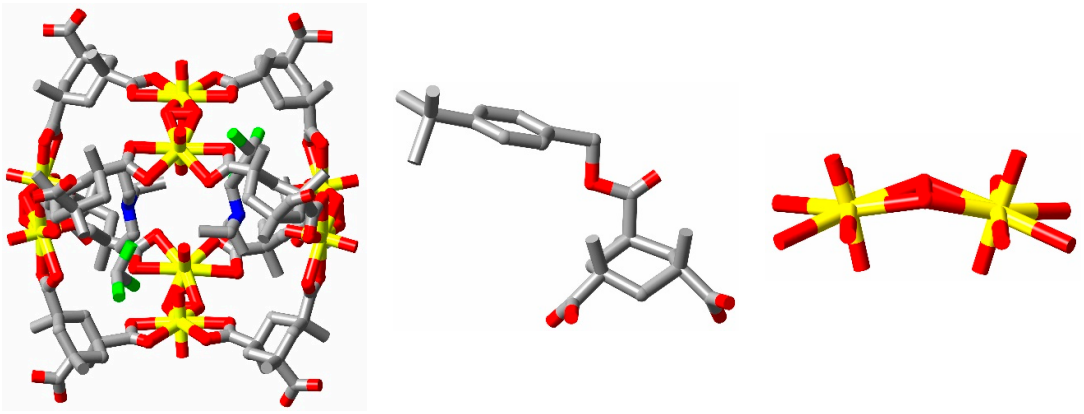

(**a**) (**b**) (**c**)

Figure 1. (**a**) A perspective view of the octa-uranate cage present in the crystal of complex **A**, showing the included triethylammonium ions and chloroform molecules but not the ester groups on the ligand; (**b**) The complete ligand, with its ester group; (**c**) The bent $O_6U(O_2)UO_6$ unit present in the complex. H-atoms were not included in the structure. (Colour code: grey = C, blue = N, red = O, green = Cl, yellow = U.)

Thus, the $[(UO_2)_8(L)_8(O_2)_4]^{8-}$ cavity must be considered unsuitable for photocatalysed oxidation reactions involving the excited UO_2^{2+} ion. The same conclusion must be drawn in relation to the octanuclear uranyl cage (Figure 2), found in the complex of composition $(HNEt_3)_8[(UO_2)_8(H_2bcat)_4(O_2)_8]\cdot 22H_2O$, (**B**, CSD refcode QAGCOR) [63], obtained with a *bis*-catechol ligand in its doubly deprotonated form (H_2bcat^{2-}). The origin of the peroxide ligands is presumably the same as that of peroxide in complex **A**, although any loss of uranyl emission (not actually demonstrated) here could be due to the phenoxide ligands, similar highly coloured but non-emissive complexes being well known for the calixarenes [64]. $(UO_2)_4(O_2)_4$ units form two bowl-shaped entities that provide caps to the cage. That the estimated internal volume [63] of the cage in **B** is less than that of the cavity in **A** may explain why only water molecules are found within and the triethylammonium counter cations are located externally, being involved in H-bonding to peroxo-O atoms.

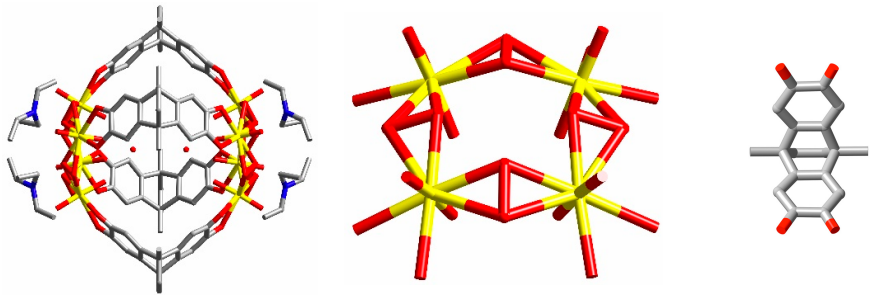

(**a**) (**b**) (**c**)

Figure 2. Perspective views of (**a**) the octanuclear cage found in the crystal of complex **B**, showing the oxygen atoms of the two included water molecules (H-atoms not located) and the external location of triethylammonium ions; (**b**) the capping unit of the cage formed by 4 uranyl ions bridged by 4 peroxide ions and (**c**) the bis(catecholate) ligand linking the capping units. H-atoms on C are not shown.

The same limitation to its utility must be applied again to the more recently described cavity-containing complex obtained through reaction of uranyl nitrate with a dicarboxylate derivative of calix[4]pyrrole ($cpdc^{2-}$) to give a product of composition

$[(UO_2)_4(cpdc)_4(O_2)_2](pyH)_4{\cdot}4dmf$, (**C**, CSD refcode IDOKIY; dmf = dimethylformamide) (Figure 3) [65]. Interestingly, the capsular form of the $[(UO_2)_4(cpdc)_4(O_2)_2]^{4-}$ anion present cannot here be attributed to the convergent nature of the $U(O_2)U$ units, since these are not centred on a common point, and must instead be a consequence of the convergent array of the carboxylate substituents of $cpdc^{2-}$. While the dimensions of the cavity in **C** are similar to those of that in **A**, with four small molecules/ions found in each cavity, in **C** the occupying species are all neutral, disordered dmf, with the pyridinium counter cations being confined to the exterior of the cavity by insertion into the calixpyrrole cups. A means of controlling the species entering an anionic cavity, differing from that seen in complex **B**, is therefore evident. In this regard, it should also be noted that the anionic capsules in **C** form stacks parallel to the *a* axis so as to define a narrow channel, a structure which could be regarded as suitable for the insertion through several capsules of a long molecular chain species or simply as a pathway for small molecule entry into the cavities. Another significant aspect of the synthesis of complex **C** is that it appears to form via the intermediacy of a photoactive $[(UO_2)_2(cpdc)_3]^{2-}$ anion, also considered likely to be capsular, though not characterised as such crystallographically. Such a capsule might be too small to be useful as a molecular flask for photo-oxidation of molecules larger than water (see ahead).

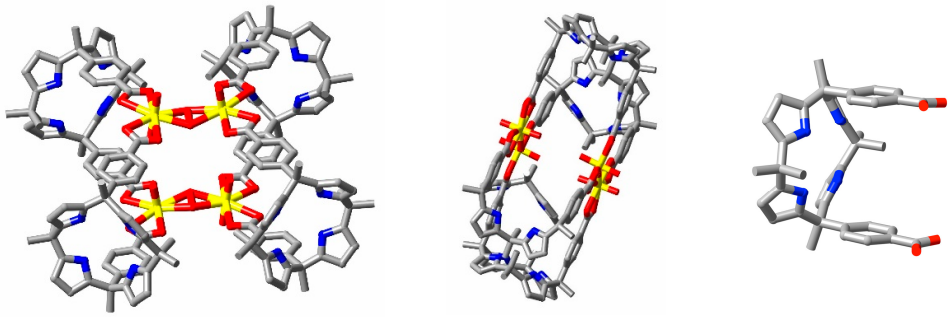

(**a**) (**b**) (**c**)

Figure 3. (**a**) A perspective view of the tetranuclear cage present in complex **C** (4 disordered dmf molecules included are not shown) showing the opposed bending of the $U(O_2)U$ units; (**b**) A view down one column of cages showing the rather constricted channel formed. (Dmf molecules, which do not block the central region of the channel, are again not shown.); (**c**) perspective view of the disubstituted calixpyrrole ligand.

The structure of complex **C** provides far from the first example of a uranyl ion complex where there are enclosed channels which might engender porosity in the crystal, a simple early example being that of the chiral tubes (Figure S1) defined by helical polymer chains in $[UO_2(dipic)(OH_2)]$ [66] (CSD refcode PYDCUO; dipic = dipicolinate = pyridine-2,6-dicarboxylate), although here it seems that the inner space of the tube is too small even to include water molecules and it is unoccupied. Many other "nanotubular" species (not all based on carboxylates) have since been characterised [47,67–76], their significance lying not only in their possible suitability as reaction vessels for the synthesis or oxidation of long, linear molecules but also, relating to the focus of the present discussion, as channels which might be used to link and provide access to capsular reaction vessels. The objective here would be the creation of uranyl ion-based structures analogous to those of zeolites and mesoporous silicas, an objective, which despite an early success [77] (discussed ahead), has been attained in but a few instances [42–44]. An intriguing comparative consideration here is that of the relationships between graphite, fullerenes, and carbon nanotubes, since a common feature of the crystal structures of anionic uranyl ion complexes of dicarboxylates is the presence of diperiodic honeycomb layers with a hexagonal form similar to that of graphite [42,47–49,78]. While the appropriate choice of ligand has certainly enabled this tendency to be overcome, the actual outcome has proved difficult to predict, as is well illustrated by various investigations of the dianion of camphoric acid as a ligand for uranyl ion [79–82].

(1*R*,3*S*)-Camphoric acid (H_2cam) is a readily available, chiral dicarboxylic acid with the desirable feature that it can provide two carboxylate groups oriented such that although they are too far apart to simply chelate a single metal ion, they can be convergently arranged so as to favour closed oligomeric complex units. Thus, a U(camphorate)U unit can adopt a form equivalent to that of the $U(O_2)U$ unit considered above, although the equivalence is inexact in that the carboxylate groups need not necessarily adopt κ^2O,O' chelation and rotation about the $C–CO_2–$ bonds can occur. In the neutral (1:1 uranyl:dicarboxylate) complex $[UO_2(cam)(py)_2]\cdot py$ (py = pyridine), (**D**, CSD refcode PENFIY) [82], the uranium is 8-coordinate with the pyridine ligands in *trans* positions and although the cam^{2-} ligands bind as bis(κ^2O,O') chelates and have a convergent form, they are only present in sufficient number to link uranyl centres into chains or rings. Thus, what is found is that the complex is a 1D zig-zag polymer (Figure 4a) rather than a metallacycle, perhaps as a consequence of the pyridine ligands forcing the carboxylate units to be as remote as possible in the uranium coordination sphere. With methanol as the co-ligand rather than pyridine in $[UO_2(cam)(CH_3OH)]\cdot CH_3OH$, (**E**, CSD refcode PENFOE), the uranium is now 7-coordinate and the crystal contains diperiodic sheets involving fused 8- and 32-membered metallacyclic units where each cam^{2-} binds to three uranium centres with one carboxylate forming a κ^2O,O' chelate and the other forming a μ^2-κ^1O,κ^1O' bridge (Figure 4b). Since the cam^{2-} conformation is very similar in both complexes, it is apparent that this cannot be the only factor controlling the structures. One obvious additional influence is the coordination mode of the carboxylate units, as well-exemplified in the 1:1 complexes of uranyl ion with cyclobutane-1,1-dicarboxylate, where both 4- and 6-membered chelate rings form part of a simple binuclear species (CSD refcode PENFEU) [82], and with (2*R*,3*R*,4*S*,5*S*)-tetrahydrofurantetracarboxylate, where 7-membered chelate rings are found in metallamacrocyclic oligomers possibly of sufficient depth to accommodate small molecules (CSD refcodes IZOHEK and IZOHIO) [83].

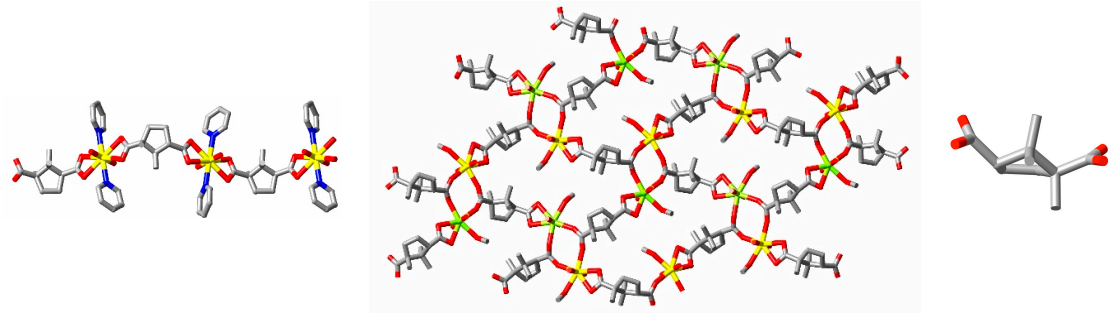

(**a**) (**b**) (**c**)

Figure 4. (**a**) Section of the monoperiodic chains found in the crystal of complex **D**; (**b**) partial view of the diperiodic sheet found in the crystal of complex **E**; (**c**) perspective view of the camphorate ligand present in both.

When uranyl ion and H_2cam are reacted in the presence of 1,4-diazabicyclo[2.2.2]octane (DABCO), however, the bent arrangement does appear to have the desired effect in that in the crystal of $[(UO_2)_8\{(cam)_{12}H_8\}]\cdot 12H_2O$, (**F**, CSD refcode MUNKOW), an octanuclear cage species (Figure 5a) with both carboxylate groups bound in the 4-membered, κ^2O,O' chelate mode, is found [81]. This chiral cage has quite large portals and its packing in the crystal results in facing arrays which define channels indicating it might well have 3-dimensional porosity, although this property has not been established. As a neutral species, the cage might be expected to be able to encapsulate neutral small molecules but the resolved water molecules of the structure are found either on the faces of the cages or in between cages, where H-bond acceptor sites are most abundant. That the cage has significant stability is indicated by the fact that it can be crystallised in its fully deprotonated form as Ba(II) [81] and K(I) [80] derivatives (CSD refcodes MUNKUC and LIYRAO), although here the channels are now blocked by the counter cations. This could mean, nonetheless, that the complexes might be used as ion-exchange materials but the fact that in the presence of NH_4^+ and

$CH_3PPh_3^+$ cations, camphoric acid and uranyl ion react [79] to give crystals of composition $[CH_3PPh_3]_3[NH_4]_3[(UO_2)_6(cam)_9]$, (**G**) (CSD refcode JIVBOI), containing a hexanuclear cage complex (Figure 5b) in which a phosphonium cation occupies the cage, indicates that any such capacity would be limited. It also must be noted that although luminescence measurements have not been made on all these complexes, where they have [79,80], uranyl ion emission appears to be largely, if not completely quenched, indicating a limited potential for photo-oxidation catalysis. In some instances, while uranyl ion emission is not observed or is weak, broad-band emission of obscure origin is observed, providing yet another indication that the photophysics of uranyl ion complexes in the solid state is yet to be fully understood [61,84,85].

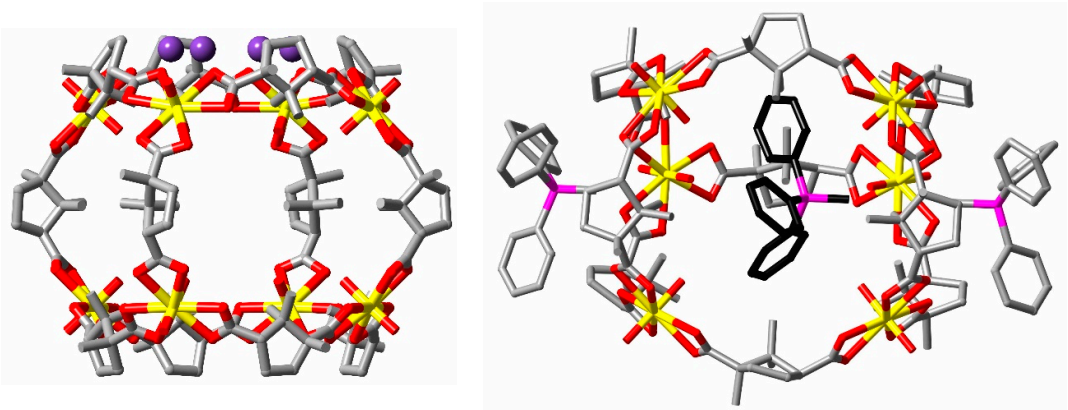

(**a**) (**b**)

Figure 5. Perspective views of (**a**) the octanuclear cage found in the crystal of complex **F**, with the oxygen atoms of water molecules (H-atoms not located) associated with a cage portal shown as violet spheres); (**b**) the hexanuclear cage, with associated $[MePPh_3]^+$ cations, found in the crystal of complex **G** (P atoms in violet; carbon atoms of the included cation are shown in black).

Structural characterisation [86–89] of uranyl ion complexes of dicarboxylate ligands rather closely related to camphorate, adamantane-1,3-dicarboxylate (adc^{2-}) and adamantane-1,3-diacetate (ada^{2-}) has further exposed the variety of influences determining their nature in the solid state. Thus, the ligand with the closer similarity to camphorate, adc^{2-}, reacts with uranyl ion in a 1.5:1 (ligand:metal) ratio to give not a closed, cage complex but a triperiodic network, of composition $[H_2NMe_2]_2[(UO_2)_2(adc)_3]\cdot 1.5H_2O$, (**H**, CSD refcode ZOZCIC), in which channels (Figure S2) are occupied by dimethylammonium cations (formed by hydrolysis of the dimethylformamide cosolvent), even though the ligand is again bound in a *bis*(κ^2O,O') mode [89]. When Cu(II) replaces the dimethylammonium cations, a triperiodic network is again formed but it is one involving diperiodic polymers of $[(UO_2)_2(adc)_3]^{2-}$ units linked by Cu(II) bridges involving Cu–O(carboxylate) bonding which disrupts the uranyl-carboxylate interactions, so that the ligands function only as *bis*(κ^1O) donors to uranium (CSD refcode ZOZDID). The effects of other metal ions on uranyl-carboxylate complex structures are so varied as to require separate analysis but one untoward effect which must be noted here is that it is common to find that the presence of the hetero-metal ion leads to quenching of uranyl ion emission [61,85,90,91], as in fact is complete in the present instance probably because of the close proximity of the Cu and U centres. With ada^{2-}, a complex of similar stoichiometry to **H**, of composition $[H_2NMe_2]_2[(UO_2)_2(ada)_3]\cdot 1.5H_2O$, (**I**, CSD refcode IHOGIX) [88], can be isolated in which sheets of rather convoluted diperiodic polymer (Figure S3) are present, with the conformational freedom resulting from the presence of the CH_2–CO_2– bonds seemingly allowing the carboxylate units of one ligand unit to adopt more divergent relative orientations than those in the adc^{2-} units of **H**, even though the ligand is bound as a *bis*(κ^2O,O') species. In the complex $[H_2NMe_2][PPh_3Me][(UO_2)_2(ada)_3]\cdot H_2O$, (**J**, CSD refcode YEXDIR) [87], where methyltriphenylphosphonium has replaced one dimethylammonium cation of **I**, one of the 3 inequivalent units adopts a completely divergent arrangement of its carboxylate

groups and diperiodic polymer sheets with a distorted honeycomb topology (Figure S4) are formed, all three ligand units still being bound in the *bis*(κ²*O,O′*) mode. When the (formal) ion exchange is complete for the 1:1.5 U:adc system as in $[NH_4]_2[PPh_4]_2[(UO_2)_4(ada)_6]\cdot H_2O$, (**K**, CSD refcode YEXDAJ), and $[NH_4]_2[PPh_3Me]_2[(UO_2)_4(ada)_6]\cdot H_2O$, (**L**, CSD refcode YEXDEN), an essentially identical tetranuclear, metallatricyclic cage species is now found in both (Figure 6). Of the six ada^{2-} ligands in a cage, four have a convergent array of carboxylates and two a divergent array, although all six behave as *bis*(κ²*O,O′*) chelates. While the ammonium ions are H-bonded to the exterior of the cage, the phosphonium cations and particularly the $[PPh_3Me]^+$ species partly occupy the interior through CH···O interactions and it is not evident that the cage could accommodate other molecules or that any exchange could occur without transformation of the cage. The dependence of the structure of complexes based on 1:1.5 uranyl:ligand units on the counter cation is further illustrated in the structures [86] of $[PPh_4]_2[(UO_2)_2(adc)_3]\cdot 2H_2O$, (**M**) (CSD refcode GOTPAJ), and $[PPh_4]_2[(UO_2)_2(ada)_3]$, (**N**) (CSD refcode GOTPIR), where very similar 1D, trough-like polymers (Figure S5) are present. The cavities defined by these troughs are occupied by the counter cations, so that once again, although these complexes are like other monometallic uranyl complexes of both adc^{2-} and ada^{2-} in showing uranyl ion luminescence, they do not offer any obvious prospect of being useful for photo-oxidation catalysis.

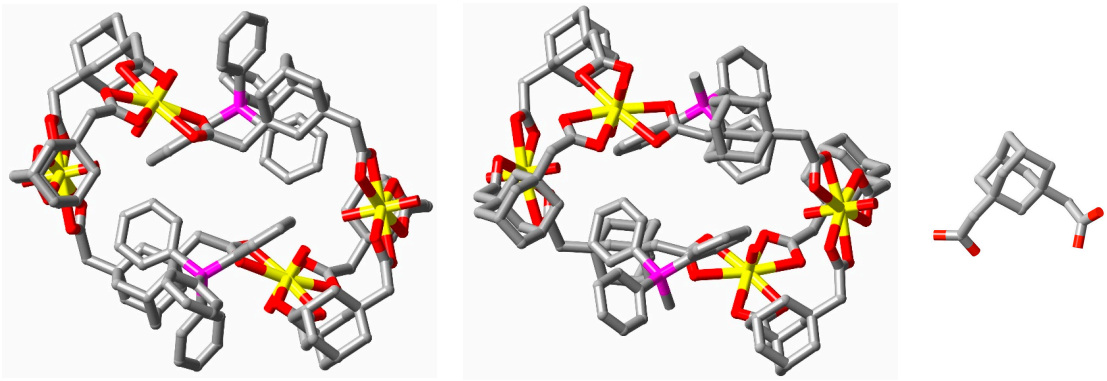

(**a**) (**b**) (**c**)

Figure 6. The near identical macrotricyclic, tetranuclear cages, along with their nearest phosphonium cations, found in the crystals of (**a**) complex **K** and (**b**) complex **L**; (**c**) one conformation of the adc^{2-} ligand found in these complexes.

Where conformational restrictions are somewhat diminished compared to camphor or adamantane derivatives in the *cis* and *trans* isomers of 1,2-cyclohexane dicarboxylates $ccdc^{2-}$ and $tcdc^{2-}$), tetrahedral cage species based on UO_2(κ²*O,O′*-carboxylate)$_3$ apices have been obtained for the *trans* isomer and an octanuclear cage for the *cis* (complexes **O** and **P**, Figure 7, CSD refcodes WANKAA and LICNIX, respectively) [92–94]. Broader investigations [95–97] of the uranyl ion complexes of these ligands have shown that these particular results are due to the choice of counter cation for the anionic oligomers, although the range is quite wide for the tetranuclear cages from the *trans* isomer and it has been suggested that the cage may be the favoured form for the stoichiometry 1:1.5 U:ligand [92]. These tetranuclear cages are luminescent and uranyl-O atoms, potentially sites for photoreaction [21], are directed towards the interior, but the internal space of the cage is too small to accommodate any molecule of real interest. The octanuclear cage derived from the *cis* isomer has a near-cubic array of U centres with one oxygen on each directed towards the interior and four involved in H-bonds to an encapsulated ammonium ion, and could be expected to be suitable for the inclusion of small molecules, although unfortunately it shows very weak luminescence.

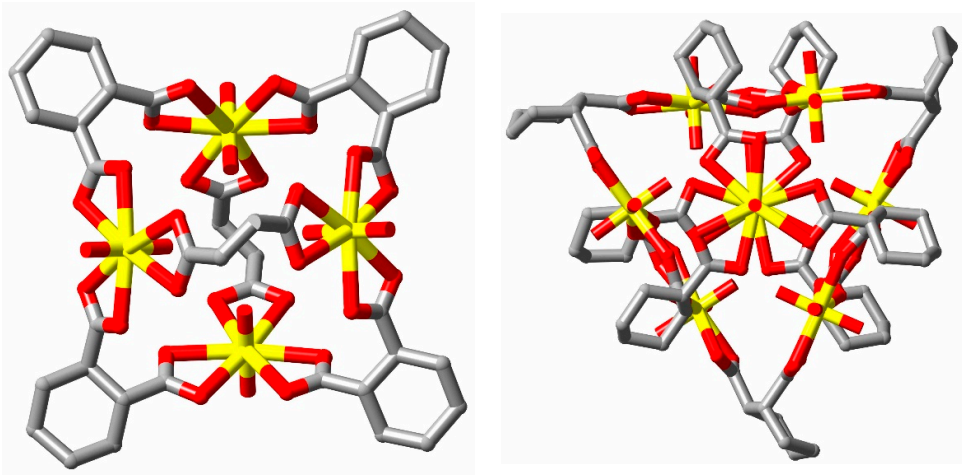

(**a**) (**b**)

Figure 7. Views (**a**) of the tetranuclear, tetrahedral cluster found in the structure of $[NH_4]_4[(UO_2)_4(tcdc)_6]$, **O** and (**b**) the octanuclear, near-cubic cage found in the structure of $[NH_4][PPh_4][(UO_2)_8(ccdc)_9(H_2O)_6]\cdot 3H_2O$, **P**.

Although the examples given above show that conformational restrictions in dicarboxylate ligands do have some influence on the structure of their uranyl ion complexes, it is worthy of note that even conformationally highly flexible aliphatic α,ω-dicarboxylates [98,99], which typically give diperiodic coordination polymers [98], can be induced to form anionic cage oligomers of helical form (helicates) in the presence of particular counter cations [99]. Thus, in the presence of $[Co(bipy)_3]^{2+}$ or $[Ni(bipy)_3]^{2+}$ (bipy = 2,2′-bipyridine), uranyl ion and 1,7-heptanedicarboxylic acid (H_2C9) react to give isomorphous crystals of composition $[M(bipy)_3][(UO_2)_2(C9)_3]$ (M = Co and Ni, CSD refcodes DACGIA and DACGOG, respectively), while with $[Mn(phen)_3]^{2+}$ or $[Co(phen)_3]^{2+}$ (phen = 1,10-phenanthroline) and 1,10-decanedicarboxylic acid (H_2C12), isomorphous $[M(phen)_3][(UO_2)_2(C12)_3]$ crystals result (**Q**, CSD refcodes DACGUM and DACHAT for Mn and Co, respectively). The anionic capsules present (Figure 8) are small, with an internal space partly occupied by the aza-aromatic ligands on the counter cations and with little space for any guest. As the U···U separations (~7.5 Å) in these species are very close to that in complex **C** described above, this is taken as an indication that the supposed $[(UO_2)_2(cpdc)_3]^{2-}$ precursor to **C** would also lack the capacity to act as a reaction vessel.

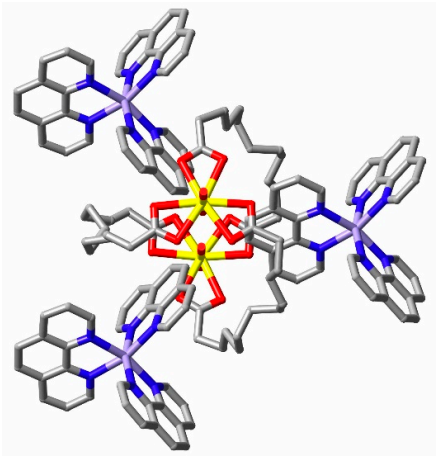

Figure 8. Perspective view of the binuclear, triple-stranded, anionic helicate and associated cations found in the crystal of $[Mn(phen)_3][(UO_2)_2(C12)_3]$, one of the isomorphous complexes **Q**. (Violet =

Mn; C12 = 1,10-dodecanedicarboxylate; H-atoms and partial disorder of the polymethylene chains are not shown.)

Recognition of the fact that four carboxylate groups disposed on a scaffold such that they are tetrahedrally oriented provide two orthogonal, bent dicarboxylate entities leads to the expectation that an appropriate such ligand could be used to provide linked cavities within a triperiodic framework polymer. This expectation was first realised (fortuitously) in the synthesis of the uranyl ion complex of the *trans*,*trans*,*trans* isomer of 1,2,3,4-cyclobutanetetracarboxylate ($cbtc^{4-}$) formed from its *cis*,*trans*,*cis* isomer under solvothermal conditions [77]. Thus, the structure of the complex $[H_3O]_2[(UO_2)_5(cbtc)_3(H_2O)_6]$, (**R**, CSD refcode GOJFAN), contains octanuclear boxes (Figure 9), where each uranyl centre is bound by three κ^2O,O' carboxylate units, linked by tetranuclear metallacycles where each uranyl centre is bound to two κ^2O,O' carboxylate units and two water molecules (in *trans* positions). Neither the luminescence nor porosity of complex **R**, nor of the more recently isolated framework complex $[H_2NMe_2]_4[(UO_2)_4(cbtc)_3]$ (similar but of a different topological type, CSD refcode TOJJAG) [100], have yet been studied but certainly the porosity of the uranyl ion complexes of *tetrakis*(4-carboxyphenyl)methane, where a single atom is the source of the tetrahedral orientation, has been demonstrated [42]. It is of course not essential that dicarboxylate units be orthogonally directed in order to generate triperiodic structures of linked cavities, as is seen in the formation of such structures with *cis*,*trans*,*cis*-cyclobutanetetracarboxylate [77] and in the more recently studied structures of uranyl ion complexes of porphyrin-derived tetracarboxylates [39] (where photoreactivity is associated with the porphyrin centres).

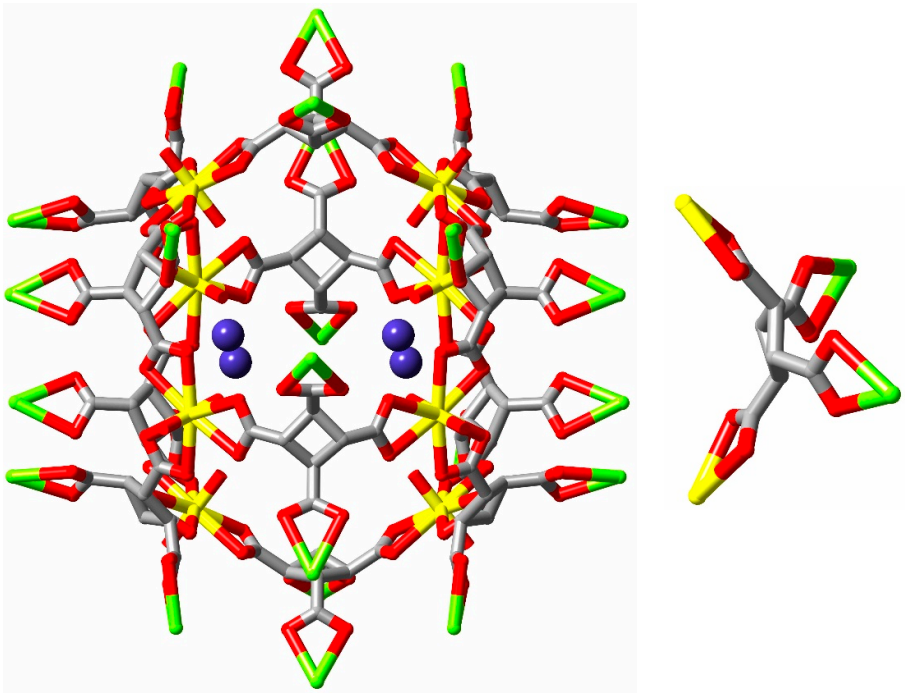

(**a**) (**b**)

Figure 9. (**a**) Perspective view of the box-like unit, defined by the uranium atoms shown in yellow, and linked to others through tetranuclear metallacyclic units (not shown) involving the uranium atoms shown in green, found in the crystal of complex **R**. Water molecule oxygen atoms within the box are shown in violet; (**b**) the tetrahedral array produced by the *trans*,*trans*,*trans* conformation of the ligand.

That convergent polycarboxylates can be used as well to generate capsular structures is beautifully demonstrated by the structures of the complexes formed by calix[4]- and calix[5]-arene carboxylates (e.g., structures **S**, Figure 10, CSD refcodes YANGUR and YANHAY, respectively)

[101]. The cavities formed here are large and can accommodate species as big as tetraprotonated cyclen (1,4,7,10-tetra-azacyclododecane) in the case of the calix[4]arene tetracarboxylate or several pyridinium and pyridine species in the calix[5]arene pentacarboxylate derivative, where the estimated effective volume of the cavity is 7000 Å^3. Luminescence measurements are not available for these complexes and a concern is that the presence of the calixarene units may lead to quenching (see above). Since the capsules are anionic, it is unsurprising that they include cations but this may be a barrier to the inclusion of neutral potential substrate molecules.

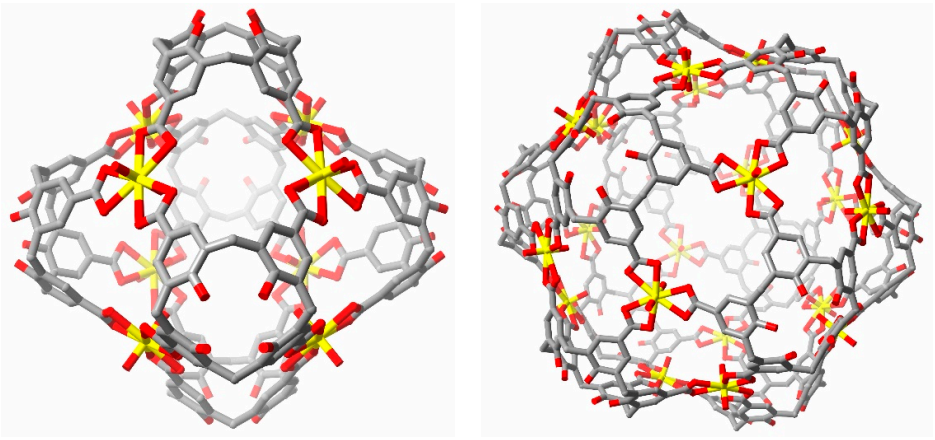

(**a**) (**b**)

Figure 10. The (**a**) octanuclear (**S1**) and (**b**) icosanuclear (**S2**) cages formed from complexation of uranyl ion by calix[4]arene tetracarboxylate and calix[5]arene pentacarboxylate, respectively. (Figures shown with depth fading of the atoms.).

Just as bent dicarboxylate units can be seen as possible struts to a uranyl ion capsule, tripodal tricarboxylates can be seen as possible caps and an obvious candidate for this role is the trianion of Kemp's triacid, *cis*,*cis*-1,3,5-trimethyl-1,3,5-cyclohexane tricarboxylic acid (H_3kta) [102], in its chair conformation where all three carboxylate groups are axially disposed. In the complex $[Ni(bipy)(OH_2)_4][(UO_2)_8(kta)_6(OH_2)_6]$, (**T**, CSD refcode POGZIW) [103], the kta^{3-} ligands do indeed sit upon the six faces of a near-cubic octanuclear anion, bridging four uranium centres as a result of two carboxylates forming κ^1O,κ^1O' bridges and one forming a κ^2O,O' chelate. Once again, the internal volume of the cage is not great and but a single water molecule, H-bonded to uranyl-O appears to be encapsulated (Figure 11). Luminescence measurements were not reported but the presence of Ni(II) in the counter cation raises the possibility that uranyl emission would be quenched, as would be expected in the case of several heterometallic compounds, some involving the same cage as just described and other larger aggregates (described in detail elsewhere [47]), characterised [104] in extension of the initial study. In a further extension [105], however, where luminescence (but not quantum yield) measurements were conducted on some similar heterometallic complexes of *cis*,*cis*-1,3,5-cyclohexanetricarboxylate (ctc^{2-}), quenching there was clearly not complete, although a factor here may have been an apparent preference for the triequatorial disposition of the carboxylates leading to the predominant formation of honeycomb-like diperiodic polymer sheets, just as indeed observed for kta^{3-} complexes involving counter cations other than $[Ni(bipy)(OH_2)_4]^{2+}$ [104,105]. Both ligands have been shown to form tubular species, with all carboxylate groups axial and additional Ni(II) cations in the case of Kemp's triacid, and with all carboxylate groups equatorial in the case of Hctc$^-$, the latter exemplifying the introduction of curvature into a honeycomb sheet precursor (CSD refcodes POHPEJ and RORROH, respectively). The trianion (kta^{3-}) is even found in a boat conformation in $M[UO_2(kta)]$ complexes ($M = H_2NMe_2$ (CSD refcode QUKLAL) or Cs) [106,107], rendering the synthesis of complexes of its triaxial chair form more a matter of chance rather than design. Nonetheless, that a tricarboxylate constrained to a discoidal form with all carboxylates oriented so as to favour a planar form of their complex does not necessarily generate diperiodic honeycomb species and in fact gives a triperiodic complex with multiple large, linked cavities is seen

in the remarkable structure of the uranyl ion complex of 1,3,5-trimethyl-2,4,6-*tris*(4′-carboxyphenyl)benzene (CSD refcode UNUNEY) [43,44].

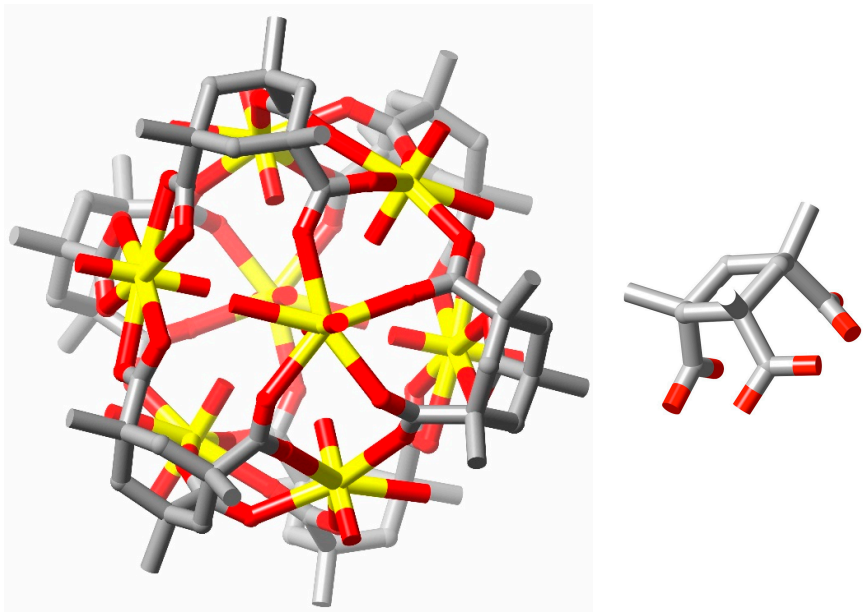

(**a**) (**b**)

Figure 11. (**a**) The octanuclear cage (again shown with depth fading) found in the crystal of complex **T**; (**b**) perspective view of the convergent triaxial conformation of the ligand found in the complex.

3. Conclusions

While the lack of complete luminescence and porosity measurements for known capsular oligomers of uranyl carboxylates creates some uncertainty as to their potential value as photo-oxidation catalysts, there seems little likelihood that any would be selective due to their capacity to encapsulate substrates of moderate molecular size. Practical aspects of application, such as stability under reaction conditions are also completely unexplored. Geometrical analysis analogous to that applied to other metallacapsule design [108,109] could of course be used along with the "extended ligand" approach [110] to prepare ligands suited to the formation of larger cavities, although this involves the danger of generating interpenetration in the structures, already seen in numerous uranyl coordination polymers [111]. Another potential drawback with most known capsules is that they are anionic and thus favour interaction with cations, so that one objective of continuing efforts of synthesis would be to couple a neutral bridging ligand, such as a bis(naphthyridine), with two carboxylate units on every uranium. The focus of this brief review has been on solid materials containing capsular species, in part because known examples are all solids of low solubility in any solvent and in part because product separation is more straightforward with heterogeneous catalysis but soluble capsular species would also be of interest. The attraction of a capsular species as a reaction vessel is that any selectivity depends on the structure of the capsule itself and not upon the environment in which it is found and capsular species which align in crystals so as to define channels, as found in various instances described herein, could offer heterogeneous catalysts of this type. Here, tubular complexes as found with selenates [71,72] and phosphonates [52–55] as well as with polycarboxylates such as tricarballylate [112], iminodiacetate [69] and phenylenediacetates [68], would also be of interest, especially if a better understanding of metal ion quenching of uranyl ion luminescence in solids could be attained, since many tubular systems are those involving heterometallic species [47]. As solvothermal synthesis [113,114] is widely applied for the isolation of crystalline uranyl ion complexes, another need is for more data concerning kinetics and equilibria of complex formation under conditions of high temperature and pressure, particularly in mixed solvents. Finally, it is essential to note that the crystal structures of known

uranyl ion complexes are frequently seen [115–118] to be sensitive to a wide range of weak interactions, so that the supramolecular behaviour of a bound ligand is a crucial aspect of its design but one yet to be mastered.

Supplementary Materials: The following are available online at www.mdpi.com/xxx/s1, Figure S1: Perspective view of one helical tube within the crystal of $[UO_2(dipic)(OH_2)]$; Figure S2: Views, down a, of the triperiodic structure of $[H_2NMe_2]_2[(UO_2)_2(adc)_3]\cdot 1.5H_2O$; Figure S3: Views of one of the diperiodic sheets found in the crystal of $[H_2NMe_2]_2[(UO_2)_2(ada)_3]\cdot 1.5H_2O$; Figure S4: Views of the diperiodic anionic polymer sheets (counter cations not shown) in the crystal of $[H_2NMe_2][PPh_3Me][(UO_2)_2(ada)_3]\cdot H_2O$; Figure S5: Views of the trough-like anionic monoperiodic polymers and their closest cations found in the crystals of (a) $[PPh_4]_2[(UO_2)_2(adc)_3]\cdot 2H_2O$ and (b) $[PPh_4]_2[(UO_2)_2(ada)_3]$.

Funding: This research received no external funding.

Conflicts of Interest: The authors declare no conflict of interest.

References and Notes

1. Kaneko, K.; Rodríguez-Reinoso, F. (Eds) *Nanoporous Materials for Gas Storage. Green Energy and Technology*; Springer: Singapore, 2019.
2. Fang, Y.; Powell, J.A.; Li, E.; Wang, Q.; Perry, Z.; Kirchon, A.; Yang, X.; Xiao, Z.; Zhu, C.; Zhang, L.; et al. Catalytic reactions within the cavity of coordination cages. *Chem. Soc. Rev.* **2019**, *48*, 4707–4730.
3. Wang, Y.; Wöll, C. Chemical Reactions at Isolated Single-Sites inside Metal-Organic Frameworks. *Catal. Lett.* **2018**, *48*, 2201–2222.
4. Hooley, R.J. Rings and Things: The Magic of Building Self-Assembled Cages and Macrocycles. *Inorg. Chem.* **2018**, *57*, 3497–3499 and following articles.
5. Ma, S.; Perman, J.A. (Eds) *Elaboration and Applications of Metal-Organic Frameworks*; World Scientific: Singapore, 2017.
6. Lin, Y.; Kong, C.; Zhang, Q.; Chen, L. Metal-Organic Frameworks for Carbon Dioxide Capture and Methane Storage. *Adv. Energy Mater.* **2017**, *7*, 1601296.
7. Rogge, S.M.J.; Bavykina, A.; Hajek, J.; Garcia, H.; Olivos-Suarez, A.I.; Sepulveda-Escribano, A.; Vimont, A.; Clet, G.; Bazin, P.; Kapteijn, F.; et al. Metal-organic and covalent organic frameworks as single-site catalysts. *Chem. Soc. Rev.* **2017**, *46*, 3134–3184.
8. Gao, C.; Wang, J.; Xu, H.X.; Xiong, Y.J. Coordination chemistry in the design of heterogeneous photocatalysts. *Chem. Soc. Rev.* **2017**, *46*, 2799–2823.
9. Huang, Y.B.; Liang, J.; Wang, X.S.; Cao. R. Multifunctional metal-organic framework catalysts: Synergistic catalysis and tandem reactions. *Chem. Soc. Rev.* **2017**, *46*, 126–157.
10. Zhu, L.; Liu, X.Q.; Jiang, H.L.; Sun, L.B. Metal-Organic Frameworks for Heterogeneous Basic Catalysis. *Chem. Rev.* **2017**, *117*, 8129–8176.
11. Zhuang, J.L.; Terfort, A.; Wöll, C. Formation of oriented and patterned films of metal-organic frameworks by liquid phase epitaxy: A review. *Coord. Chem. Rev.* **2016**, *307*, 391–424.
12. Liu, J.W.; Chen, L.F.; Cui, H.; Zhang, J.Y.; Zhang, L.; Su, C.Y. Applications of metal-organic frameworks in heterogeneous supramolecular catalysis. *Chem. Soc. Rev.* **2014**, *43*, 6011–6061.
13. Cook, T.R.; Zheng, Y.-R.; Stang, P.J. Metal-Organic Frameworks and Self-Assembled Supramolecular Coordination Complexes: Comparing and Contrasting the Design, Synthesis and Functionality of Metal-Organic Materials. *Chem. Rev.* **2013**, *113*, 734–777.
14. Suh, M.P.; Park, H.J.; Prasad, T.K.; Lim, D.-W. Hydrogen Storage in Metal-Organic Frameworks. *Chem. Rev.* **2012**, *112*, 782–835.
15. Inokuma, Y.; Kawano, M.; Fujita, M. Crystalline Molecular Flasks. *Nature Chem.* **2011**, *3*, 349–358.
16. Kapelewski, M.T.; Runčevski, T.; Tarver, J.D.; Jiang, H.Z.H.; Hurst, K.E.; Parilla, P.A.; Ayala, A.; Gennett, T.; Fitzgerald, S.A.; Brown, C.M.; et al. Record High Hydrogen Storage Capacity in the Metal-Organic Framework Ni_2(*m*-dobc) at Near-Ambient Temperature. *Chem. Mater.* **2018**, *30*, 8179–8189.
17. Sumida, K.; Rogow, D.L.; Mason, J.A.; McDonald, T.M.; Bloch, E.D.; Herm, Z.R.; Bae, T.-H.; Long, J.R. Carbon Dioxide Capture in Metal-Organic Frameworks. *Chem. Rev.* **2012**, *112*, 724–781.
18. Hoshino, M.; Khutia, A.; Xing, H.; Inokuma, Y.; Fujita, M. The crystalline sponge method updated. *IUCr J.* **2016**, *3*, 139–151.

19. Gee, W.J. The growing importance of crystalline molecular flasks and the crystalline sponge method. *Dalton Trans* **2017**, *46*, 15979–15986.
20. Sarakha, M.; Bolte, M.; Burrows, H.D. Electron-Transfer Oxidation of Chlorophenols by Uranyl Ion Excited State in Aqueous Solution. Steady-State and Nanosecond Flash Photolysis Studies. *J. Phys. Chem. A* **2000**, *104*, 3142–3149.
21. Burrows, H.D.; Kemp, T.J. The Photochemistry of the Uranyl Ion. *Chem. Soc. Rev.* **1974**, *3*, 139–165.
22. Yusov, A.B.; Shilov, V.P. Reduction of the photo-excited uranyl ion by water. *Russ. Chem. Bull.* **2000**, *49*, 285–290.
23. Deng, X.; Li, Z.; Garcia, H. Visible Light Induced Organic Tranformations over Metal-Organic-Frameworks (MOFs). *Chem. Eur. J.* **2017**, *28*, 11189–11209.
24. Wang, Q.; Gao, Q.; El-Anizi, A.M.; Nafady, A.; Ma, S. Recent advances in MOF-based photocatalysis: Environmental remediation under visible light. *Inorg. Chem. Front.* **2020**, *7*, 300–339.
25. Khandan, F.M.; Afzali, D.; Sargazi, G.; Gordan, M. Novel uranyl-curcumin-MOF photocatalysts with high-performance photocatalytic activity toward the degradation of phenol red from aqueous solution: Effective synthesis route, design and a controllable systematic study. *J. Mater. Sci.: Mater. Electron.* **2018**, *29*, 18600–18613.
26. Li, H.-H.; Zeng, X.-H.; Wu, H.-Y.; Jie, X.; Zheng, S.-T.; Chen, Z.-R. Incorporating Guest Molecules into Honeycomb Structures Constructed from Uranium(VI) Polycarboxylates: Structural Diversity and Photocatalytic Activity for the Degradation of Organic Dyes. *Cryst. Growth Des.* **2015**, *15*, 10–13.
27. Yang, W.; Tiang, W.-G.; Liu, X.-X.; Wang, L.; Sun, Z.-M. Syntheses, Structures, Luminescence and Photocatalytic Properties of a Series of Uranyl Coordination Polymers *Cryst. Growth Des.* **2014**, *14*, 5904–5911.
28. Hou, Y.-N.; Xu, X.-T.; Xing, N.; Bai, F.-Y.; Duan, S.-B.; Sun, Q.; Wei, S.-Y.; Shi, Z.; Zhang, H.-Z.; Xing, Y.-H. Photocatalytic Application of 4f-5f Inorganic-Organic Frameworks: Influence of the Lanthanide Contraction on the Structure and Functional Properies of Uranyl-Lanthanide Complexes. *ChemPlusChem* **2014**, *79*, 1304–1315.
29. Kolinko, P.A.; Fillipov, T.N.; Kozlov, D.V.; Parmon, V.N. Ethanol vapour photocatalytic oxidation with uranyl-modified titania under visible light: Comparison with silica and alumina. *J. Photochem. Photobiol. A: Chem.* **2012**, *250*, 72–77.
30. Wang, K.-X.; Chen, J.-S. Extended Structures and Physicochemical Properties of Uranyl-Organic Compounds *Acc. Chem. Res.* **2011**, *44*, 531–540.
31. Krishna, V.; Kamble, V.S.; Gupta, N.M.; Selvam, P. Uranyl-Anchored MCM-41 as a Highly Efficient Photocatalyst in the Oxidative Destruction of Short-Chain Linear Alkanes: An in-situ FTIR Study. *J. Phys. Chem. C* **2008**, *112*, 15832–15843.
32. Liao, Z.-L.; Li, G.-D.; Bi, M.-H.; Chen, J.-S. Preparation, Structures and Photocatalytic Properies of Three New Uranyl-Organic Assembly Compounds. *Inorg. Chem.* **2008**, *47*, 4844–4853.
33. Yu, Z.-T.; Liao, Z.-L.; Jiang, Y.-S.; Li, G.-H.; Chen, J.-S. Water Insoluble Ag-U-Organic Assemblies with Photocatalytic Activity. *Chem. Eur. J.* **2005**, *11*, 2642–2650.
34. Nieweg, J.A.; Lemma, K.; Trewyn, B.G.; Lin, V.S.-Y.; Bakac, A. Mesoporous Silica-Supported Uranyl: Synthesis and Photoreactivity. *Inorg. Chem.* **2005**, *44*, 5641–5648 and references therein.
35. H. D. Burrows, M. da G. Miguel. Applications and limitations of uranyl ion as a photophysical probe. *Adv. Coll. Interf. Sci.* **2001**, *89-90*, 485–496 and references therein.
36. D. Zhang, T.K. Ronson, J.R. Nitschke. Functional Capsules via Subcomponent Self-Assembly. *Acc. Chem. Res.* **2018**, *51*, 2423–2436.
37. Yoshizawa, M.; Tamura, M.; Fujita, M. Diels-Alder in Aqueous Molecular Hosts: Unusual Regioselectivity and Efficient Catalysis. *Science* **2006**, *312*, 251–254.
38. Fiedler, D.; Leung, D.H.; Bergman, R.G.; Raymond, K.N. Selective Molecular Recognition, C–H Bond Activation and Catalysis in Nanocale Reaction Vessels. *Acc. Chem. Res.* **2005**, *38*, 351–360.
39. Shao, L.; Zhai, F.; Wang, Y.; Yue, G.; Li, Y.; Chu, M.; Wang, S. Assembly of porphyrin-based uranium organic frameworks with (3,4)-connected *pto* and *tbo* topologies. *Dalton Trans* **2019**, *48*, 1595–1598.
40. Hu, K.-Q.; Huang, Z.-W.; Zhang, Z.-H.; Mei, L.; Qian, B.-B.; Yu, J.-P.; Chai, Z.-F.; Shi, W.-P. Actinide-based Porphyrinic MOF as Dehydrogenation Catalyst. *Chem. Eur. J.* **2018**, *24*, 16766–16769.
41. Hu, F.; Di, Z.; Lin, P.; Huang, P.; Wu, M.; Jiang, F.; Hong, M. An Anionic Urnaium-Based Metal-Organic Framework with Ultralarge Nanocages for Selective Dye Adsorption. *Cryst. Growth Des.* **2018**, *18*, 576–580.

42. Hu, K.-Q.; Jiang, X.; Wang, C.-Z.; Mei, L.; Xie, Z.-N.; Tao, W.-Q.; Zhang, X.-L.; Chai, Z.-F.; Shi, W.-Q. Solvent-dependent Synthesis of Porous Anionic Uranyl-organic Frameworks Featuring Highly Symmetrical (3,4)-connected *ctn* or *bor* Topology for Selective Dye Adsorption. *Chem. Eur. J.* **2017**, *23*, 529–532.
43. Li, P.; Vermeulen, N.A.; Malliakas, C.D.; Gomez-Gualdron, D.A.; Howarth, A.J.; Mehdi, B.L.; Dohnalkova, A.; Browning, N.D.; O'Keeffe, M.; Farha, O.A. Bottom-up construction of a superstructure in a porous uranium-organic crystal. *Science* **2017**, *356*, 624–627.
44. Li, P.; Vermeulen, N.A.; Gong, X.R.; Malliakas, C.D.; Stoddart, J.F.; Hupp, J.T.; Farha, O.K. Design and synthesis of a water-stable anionic uranium-based metal–organic framework (MOF) with ultra large pores. *Angew. Chem., Int. Ed.* **2016**, *128*, 10514–10518.
45. Wang, Y.; Liu, Z.; Li, Y.; Bai, Z.; Liu, W.; Wang, Y.; Xu, X.; Xiao, C.; Sheng, D.; Diwu, J.; et al. Umbellate Distortions of the Uranyl Coordination Environment Result in a Stable and Porous Polycatenated Framework that can Effectively Remove Cesium from Aqueous Solutions. *J. Am. Chem. Soc.* **2015**, *137*, 6144–6147.
46. Ahmad, N.; Chugtai, A.H.; Younus, H.A.; Verpoort, F. Discrete metal-carboxylate self-assembled cages: Design, synthesis and applications. *Coord. Chem. Rev.* **2014**, *280*, 1–27.
47. Thuéry, P.; Harrowfield, J. Recent advances in structural studies of heterometallic uranyl-containing coordination polymers and polynuclear closed species. *Dalton. Trans*. **2017**, *46*, 13660–13667.
48. Su, J.; Chen, J.-S. MOFs of Uranium and the Actinides. *Struct. Bond. (Berlin)* **2015**, *163*, 265–296.
49. Loiseau, T.; Mihalcea, I.; Henry, N.; Volkringer, C. The crystal chemistry of uranium carboxylates. *Coord. Chem. Rev.* **2014**, *266–267*, 69–109.
50. Andrews, M.B.; Cahill, C.L. Uranyl-Bearing Hybrid Materials: Synthesis, Speciation and Solid State Structures. *Chem. Rev.* **2013**, *113*, 1121–1136.
51. Giesting, P.A.; Burns, P.C. Uranyl-organic complexes: structure symbols, classification of carboxylates, and uranyl polyhedral geometries. *Crystallogr. Rev.* **2006**, *12*, 205–255.
52. Zheng, T.; Wu, Q.-Y.; Gao, Y.; Gui, D.; Qiu, S.; Chen, L.; Sheng, D.; Diwu, J.; Shi, W.-Q.; Chai, Z.; et al. Probing the Influence of Phosphonate Bonding Modes to Uranium(VI) on Structural Topology and Stability: A Complementary Experimental and Computational Investigation. *Inorg. Chem.* **2015**, *54*, 3864–3874.
53. Yang, W.; Yi, F.-Y.; Tian, T.; Tian, W.-G.; Sun, Z.-M. Structural Variation within Heterometallic Uranyl Hybrids based on Flexible Alkyldiphosphonate Ligands. *Cryst. Growth Des.* **2014**, *14*, 1366–1374.
54. Parker, T.G.; Cross, J.M.; Polinski, M.J.; Liu, J.; Albrecht-Schmitt, T.E. Ionothermal and Hydrothermal Flux Syntheses of Five New Uranyl Phosphonates. *Cryst. Growth Des.* **2014**, *14*, 228–235.
55. Tian, T.; Yang, W.; Wang, H.; Dang, S.; Sun, Z.-M. Flexible Diphosphonic Acids for the Isolation of Uranyl Hybrids with Heterometallic U(VI)=O–Zn(II) Cation-Cation Interactions. *Inorg. Chem.* **2013**, *52*, 8288–8290.
56. Thuéry, P.; Nierlich, M.; Baldwin, B.W.; Komatsuzaki, N.; Hirose, T. A metal-organic molecular box obtained from self assembling around uranyl ions. *J. Chem. Soc. Dalton Trans* **1999**, 1047–1048.
57. McGrail, B.T.; Pianowski, L.S.; Burns, P.C. Photochemical Water Oxidation and Origin of Nonaqueous Uranyl Peroxide Complexes. *J. Am. Chem. Soc*. **2014**, *136*, 4797–4800.
58. Thangavelu, S.G.; Cahill, C.L. Uranyl-Promoted Peroxide Generation: Synthesis and Characterisation of Three Uranyl Peroxo $[(UO_2)_2(O_2)]$ Complexes. *Inorg. Chem*. **2015**, *54*, 4208–4221.
59. Qiu, J.; Burns, P.C. Clusters of Actinides with Oxide, Peroxide or Hydroxide Bridges. *Chem. Rev.* **2013**, *113*, 1097–1120.
60. Qiu, J.; Ling, J.; Jouffret, L.; Thomas, R.; Szymanowski, J.E.S.; Burns, P.C. Water soluble multi-cage super tetrahedral uranyl peroxide phosphate clusters. *Chem. Sci.* **2014**, *5*, 303–310.
61. Natrajan, L.S. Developments in the Photophysics and Photochemistry of Actinide Ions and their Coordination Compounds. *Coord. Chem. Rev.* **2012**, *256*, 1583–1603.
62. Thuéry, P.; Harrowfield, J. Anchoring Flexible Uranyl Dicarboxylate Chains through Stacking Interactions of Ancillary Ligands on the Chiral U(VI) Centres. *CrystEngComm.* **2016**, *18*, 3905–3918.
63. Thuéry, P.; Masci, B. Self Assembly of an Octa-uranate Cage Complex with a Rigid Bis-Catechol Ligand. *Supramol. Chem.* **2003**, *15*, 95–99.
64. Thuéry, P.; Nierlich, M.; Harrowfield, J.; Ogden, M. Phenoxide complexes of f-elements. In *Calixarenes 2001*; Asfari, Z., Böhmer, V., Harrowfield, J., Vicens, J., Eds.; Kluwer Academic Publishers, Dordrtecht, The Netherlands, 2001; Chapter 30, pp. 561–582.

65. Lee, J.; Brewster, J.T., II; Song, B.; Lynch, V.M.; Hwang, I.; Li, X.; Sessler, J.L. Uranyl dication mediated photoswitching of a calix[4]pyrrole-based metal coordination cage. *Chem. Commun.* **2018**, *54*, 9422–9425.
66. Immirzi, A.; Bombieri, G.; Degetto, S.; Marangoni, G. The crystal and molecular structure of pyridine-2,6-dicarboxylatodioxouranium(VI) monohydrate. *Acta Crystallogr., Sect. B: Struct. Crystallogr. Cryst. Chem.* **1975**, *31*, 1023–1028.
67. Jayasinghe, A.S.; Unruh, D.K.; Kral, A.; Libo, A.; Forbes, T.Z. Structural Features in Metal–Organic Nanotube Crystals That Influence Stability and Solvent Uptake. *Cryst. Growth Des*. **2015**, *15*, 4062–4070.
68. Thuéry, P.; Atoini, Y.; Harrowfield, J. Tubelike Uranyl–Phenylenediacetate Assemblies from Screening of Ligand Isomers and Structure-Directing Counterions. *Inorg. Chem.* **2019**, *58*, 6550–6564.
69. Unruh, D.K.; Gojdas, K.; Libo, A.; Forbes, T.Z. Development of Metal-Organic Nanotubes Exhibiting Low Temperature, Reversible Exchange of Confined "Ice Channels". *J. Am. Chem. Soc*. **2013**, *135*, 7398–7401.
70. Mihalcea, I.; Henry, N.; Loiseau, T. Revisiting the Uranyl-phthalate System: Isolation and Crystal Structures of Two Types of Uranyl-Organic Frameworks (UOF). *Cryst. Growth Des*. **2011**, *11*, 1940–1947.
71. Krivovichev, S.V.; Kahlenberg, V.; Tananaev, I.G.; Kaindl, R.; Mersdorf, E.; Myasoedov, B.F. Highly Porous Uranyl Selenate Nanotubes. *J. Am. Chem. Soc*. **2005**, *127*, 1072–1073.
72. Krivovichev, S.V.; Kahlenberg, V.; Kaindl, R.; Mersdorf, E.; Tananaev, I.G.; Myasoedov, B.F. Nanoscale tubules in uranyl selenates. *Angew. Chem. Int. Ed*. **2005**, *44*, 1134–1136.
73. Aranda, M.A.G.; Cobeza, A.; Bruque, S.; Poojary, D.M.; Clearfield, A. Polymorphism and Phase Transition in Nanotubular Uranyl Phenylphosphonate: $(UO_2)_3(HO_3PC_6H_5)_2(O_3PC_6H_5)_2.H_2O$. *Inorg. Chem.* **1998**, *37*, 1827–1832.
74. Grohol, D.; Clearfield, A. Alkali-Ion-Catalysed Transformation of Two Linear Uranyl Phosphonates into a Tubular One. *J. Am. Chem. Soc.* **1997**, *119*, 9301–9302.
75. Poojary, D.M.; Cabeza, A.; Aranda, M.A.G.; Bruque, S.; Clearfield, A. Structure Determination of a Complex Tubular Uranyl Phenylphosphonate, $(UO_2)_3(HO_3PC_6H_5)_2(O_3PC_6H_5)_2.H_2O$, from Conventional X-ray Powder Diffraction Data. *Inorg. Chem.* **1996**, *35*, 1468–1473.
76. Poojary, D.M.; Grohol, D.; Clearfield, A. Synthesis and X-ray Powder Structure of a Novel Porous Uranyl Phenylphosphonate Containing Unidimensional Channels Flanked by Hydrophobic Regions. *Angew. Chem. Int. Ed.* **1995**, *34*, 1508–1510.
77. Thuéry, P.; Masci, B. Uranyl-Organic Frameworks with 1,2,3,4-Butanetetracarboxylate and 1,2,3,4-Cyclobutanetetracarboxylate Ligands. *Cryst. Growth Des.* **2008**, *8*, 3430–3436.
78. Cahill, C.L.; Borkowski, L.A. *Structural Chemistry of Inorganic Actinide Compounds*; Krivovichev, S.V., Burns, P.C., Tananaev, I.G., Eds.; Elsevier: Amsterdam, The Netherlands, 2007; Chapter 11.
79. Thuéry, P.; Atoini, Y.; Harrowfield, J. Chiral Discrete and Polymeric Uranyl Ion Complexes with (1*R*,3*S*)-(+)-Camphorate Ligands: Counterion-Dependent Formation of a Hexanuclear Cage. *Inorg. Chem.* **2019**, *58*, 870–880.
80. Thuéry, P.; Harrowfield, J.M. Chiral One- to Three-dimensional Uranyl-organic Assemblies from (1*R*,3*S*)-(+)-Camphoric acid. *CrystEngComm* **2014**, *16*, 2996–3004.
81. Thuéry, P. A Nanosized Uranyl Camphorate Cage and its Use as a Building Unit in a Metal–Organic Framework. *Cryst. Growth Des.* **2009**, *9*, 4592–4594.
82. Thuéry, P. Solvothermal Synthesis and Crystal Structure of Uranyl Complexes with 1,1-Cyclobutanedicarboxylic and (1*R*,3*S*)-(+)-Camphoric Acids—Novel Chiral Uranyl–Organic Frameworks. *Eur. J. Inorg. Chem.* **2006**, 3646–3651.
83. Thuéry, P.; Villiers, C.; Jaud, J.; Ephritikhine, M.; Masci, B. Uranyl-Based Metallamacrocycles: Tri- and Tetranuclear Complexes with (2*R*,3*R*,4*S*,5*S*)-Tetrahydrofurantetracarboxylic Acid. *J. Am. Chem. Soc.* **2004**, *126*, 6838–6839.
84. Thuéry, P.; Atoini, Y.; Harrowfield, J. Functionalized Aromatic Dicarboxylate Ligands in Uranyl-Organic Assemblies: the Cases of Carboxycinnamate and 1,2-/1,3-Phenylenedioxydiacetate. *Inorg. Chem.* **2020**, *59*, in press, and references therein.
85. Adelani, P.O.; Albrecht-Schmitt, T.E. Heterobimetallic Copper(II) Uranyl Carboxyphenylphosphonates. *Cryst. Growth Des.* **2011**, *11*, 4676–4683.
86. Thuéry, P.; Atoini, Y.; Harrowfield, J. 1,3-Adamantanedicarboxylate and 1,3-Adamantanediacetate as Uranyl Ion Linkers: Effect of Counterions, Solvents and Differences in Flexibility. *Eur. J. Inorg. Chem.* **2019**, 4440–4449.

87. Thuéry, P.; Atoini, Y.; Harrowfield, J. Closed Uranyl-Dicarboxylate Oligomers: A Tetranuclear Metallatricycle with Uranyl Bridgeheads and 1,3-Adamantanedicarboxylate Linkers**.** *Inorg. Chem.* **2018**, *57*, 7932–7939.

88. Thuéry, P.; Harrowfield, J. Solvent effects in solvo-hydrothermal synthesis of uranyl ion complexes with 1,3-adamantanediacetate. *CrystEngComm* **2015**, *17*, 4006–4018.

89. Thuéry, P.; Rivière, E.; Harrowfield, J. Uranyl- and Uranyl-3d-Block-Cation Complexes with 1,3-adamantanedicarboxylate: Crystal Structures, Luminescence and Magnetic Properties. *Inorg. Chem.* **2015**, *54*, 2838–2850.

90. Heine, J.; Müller-Buschbaum, K. Engineering metal-based luminescence in coordination polymers and metal-organic frameworks. *Chem. Soc. Rev.* **2014**, *42*, 9232–9242.

91. Thuéry, P.; Atoini, Y.; Harrowfield, J. Zero-, mono- and diperiodic uranyl ion complexes with the diphenate dianion: Influences of transition metal ion coordination and differential U^{VI} chelation. *Dalton Trans.* **2020**, *49*, 817–828.

92. Thuéry, P.; Atoini, Y.; Harrowfield, J. Counterion-Controlled Formation of an Octanuclear Uranyl Cage with *cis*-1,2-Cyclohexanedicarboxylate Ligands. *Inorg. Chem.* **2018**, *57*, 6283–6288.

93. Thuéry, P.; Harrowfield, J. Tetrahedral and cuboidal clusters in Complexes of Uranyl and Alkali or Alkaline-Earth Metal Ions with *rac*- and (1*R*,2*R*)-*trans*-1,2-Cyclohexanedicarboxylate. *Cryst. Growth Des.* **2017**, *17*, 2881–2892.

94. Thuéry, P.; Harrowfield, J. Coordination Polymers and Cage-Containing Frameworks in Uranyl Ion Complexes with rac- and (1*R*,2*R*)-trans-1,2-Cyclohexanedicarboxylates: Consequences of Chirality. *Inorg. Chem.* **2017**, *56*, 1455–1469.

95. Thuéry, P.; Harrowfield, J. $[Ni(cyclam)]^{2+}$ and $[Ni(R,S\text{-}Me_6cyclam)]^{2+}$ as Linkers or Counterions in Uranyl–Organic Species with *cis*- and *trans*-1,2-Cyclohexanedicarboxylate Ligands. *Cryst. Growth Des.* **2018**, *18*, 5512–5520.

96. Thuéry, P.; Atoini, Y.; Harrowfield, J. Crown Ethers and their Alkali Metal Ion Complexes as Assembler Groups in Uranyl–Organic Coordination Polymers with *cis*-1,3-, *cis*-1,2- and *trans*-1,2-Cyclohexanedicarboxylates. *Cryst. Growth Des.* **2018**, *18*, 3167–3177.

97. Thuéry, P.; Atoini, Y.; Harrowfield, J. Uranyl–Organic Coordination Polymers with *trans*-1,2-, *trans*-1,4- and *cis*-1,4-Cyclohexanedicarboxylates: Effects of Bulky PPh_4^+ and PPh_3Me^+ Counterions. *Cryst. Growth Des.* **2018**, *18*, 2609–2619.

98. Borkowski, L.A.; Cahill, C.L. Crystal Engineering with the Uranyl Cation I. Aliphatic Carboxylate Coordination Polymers: Synthesis, Crystal Structures, and Fluorescent Properties. *Cryst. Growth Des.* **2006**, *6*, 2241–2247.

99. Thuéry, P.; Harrowfield, J. A New Form of Triple-stranded Helicate found in Uranyl Complexes of Aliphatic α,ω-Dicarboxylates. *Inorg. Chem.* **2015**, *54*, 10539–10541.

100. Thuéry, P.; Atoini, Y.; Harrowfield, J. Favoring Framework Formation through Structure-Directing Effects in Uranyl Ion Complexes with 1,2,3,4-(Cyclo)butanetetracarboxylate Ligands. *Cryst. Growth Des.* **2019**, *19*, 4109–4120.

101. Pasquale, S.; Sattin, S.; Escudero-Adan, E.C.; Martinez-Belmonte, M.; De Mendoza, J. Giant regular polyhedra from calixarene carboxylates and uranyl. *Nature Commun.* **2012**, *3*, 785–791.

102. Kemp, D.S.; Petrakis, K.S. Synthesis and Conformational Analysis of *cis,cis*-1,3,5-Trimethylcyclohexane-1,3,5-tricarboxylic Acid. *J. Org. Chem.* **1981**, *46*, 5140–5143.

103. Thuéry, P. A Highly Adjustable Coordination System: Nanotubular and Molecular Cage Species in Uranyl Ion Complexes with Kemp's Triacid. *Cryst. Growth Des.* **2014**, *14*, 901–904.

104. Thuéry, P. Increasing Complexity in the Uranyl Ion–Kemp's Triacid System: From One- and Two-Dimensional Polymers to Uranyl–Copper(II) Dodeca- and Hexadecanuclear Species. *Cryst. Growth Des.* **2014**, *14*, 2665–2676.

105. Thuéry, P.; Harrowfield, J. Uranyl Ion Complexes with all-cis 1,3,5-Cyclohexanetricarboxylate: Unexpected Framework and Nanotubular Assemblies. *Cryst. Growth Des.* **2014**,*14*, 4214–4225

106. Thuéry, P.; Harrowfield, J. Two-dimensional assemblies in f-element ion (UO_2^{2+}, Yb^{3+}) complexes with two cyclohexyl-based polycarboxylates. *Polyhedron* **2015** *98*, 5–11.

107. Harrowfield, J.; Thuéry, P. Dipodal, Tripodal, and Discoidal Coordination Modes of Kemp's Triacid Anions. *Eur. J. Inorg. Chem.* **2020**, in press, doi:10.1002/ejic.201901249.

108. Caulder, D.; Raymond, K.N. Supermolecules by Design. *Acc. Chem. Res.* **1999**, *32*, 975–982.

109. Jansze, S.M.; Cecot, G.; Wise, M.D.; Zhurov, K.O.; Ronson, T.K.; Castilla, A.M.; Finelli, A.; Pattison, P.; Solari, E.; Scopelliti, R.; et al. Ligand Aspect Ratio as a Decisive Factor for the Self-Assembly of Coordination Cages. *J. Am. Chem. Soc.* **2016**, *138*, 2046–2054.
110. Constable, E.C. Expanded ligands—An assembly principle for supramolecular chemistry. *Coord. Chem. Rev.* **2008**, *252*, 842–855.
111. Thuéry, P.; Harrowfield, J. Uranyl Ion-Containing Polymeric Assemblies with cis/trans Isomers of 1,2-, 1,3- and 1,4-Cyclohexanedicarboxylates, Including a Helical Chain and a Sixfold-Interpenetrated Framework. *Cryst. Growth Des.* **2020**, *20*, 262–273 and references therein.
112. Thuéry, P.; Harrowfield, J. Variations on the Honeycomb Topology: from Triangular- and Square-Grooved Networks to Tubular Assemblies in Uranyl Tricarballylate Complexes. *Cryst. Growth Des.* **2017**, *17*, 963–966.
113. Demazeau, G. Solvothermal Processes: Definition, Key Factors Governing the Involved Chemical Reactions and New Trends. *Z. Naturforsch.* **2010**, *65b*, 999–1006.
114. Demazeau, G. Solvothermal reactions: An original route for the synthesis of novel materials. *J. Mater. Sci.* **2008**, *43*, 2104–2114.
115. Thuéry, P.; Atoini, Y.; Harrowfield, J. Structure-directing effects of coordinating solvents, ammonium and phosphonium counterions in uranyl ion complexes with 1,2-, 1,3- and 1,4-phenylenediacetate. *Inorg. Chem.* **2020**, *59*, 2503–2518.
116. Carter, K.P.; Kalaj, M.; Kerridge, A.; Cahill, C.L. Probing hydrogen and halogen-oxo interactions in uranyl coordination polymers: a combined crystallographic and computational study. *CrystEngComm* **2018**, *20*, 4916–4925.
117. Carter, K.P.; Kalaj, M.; Cahill, C.L. Harnessing uranyl oxo atoms via halogen bonding interactions in molecular uranyl materials featuring 2,5-di-iodobenzoic acid and N-donor capping ligands. *Inorg. Chem. Front.* **2017**, *4*, 65–78.
118. Kalaj, M.; Carter, K.P.; Cahill, C.L. Isolating Equatorial and Oxo Based Influences on Uranyl Vibrational Spectroscopy in a Family of Hybrid Materials Featuring Halogen Bonding Interactions with Uranyl Oxo Atoms. *Eur. J. Inorg. Chem.* **2017**, 4702–4713.